VLT/CRIRES science verification observations: A hint of C18O in the young brown dwarf 2M0355

Zhang, Y.; Snellen, I.A.G.; Brogi, M.; Birkby, J.L.

OPEN ACCESS

VLT/CRIRES Science Verification Observations: A hint of $C^{18}O$ in the Young Brown Dwarf 2M0355

Yapeng Zhang[1], Ignas A. G. Snellen[1], Matteo Brogi[2,3,4], and Jayne L. Birkby[5]

Published September 2022 • © 2022. The Author(s). Published by the American Astronomical Society.

Research Notes of the AAS, Volume 6, Number 9

Citation Yapeng Zhang *et al* 2022 *Res. Notes AAS* **6** 194

DOI 10.3847/2515-5172/ac9309

yzhang@strw.leidenuniv.nl

[1] Leiden Observatory, Leiden University, Postbus 9513, 2300 RA, Leiden, The Netherlands; yzhang@strw.leidenuniv.nl

[2] Department of Physics, University of Warwick, Coventry CV4 7AL, UK

[3] INAF—Osservatorio Astrofisico di Torino, Via Osservatorio 20, I-10025 Pino Torinese, Italy

[4] Centre for Exoplanets and Habitability, University of Warwick, Gibbet Hill, Coventry, CV4 7AL, UK

[5] Astrophysics, University of Oxford, Denys Wilkinson Building, Keble Road, Oxford OX1 3RH, UK

Yapeng Zhang https://orcid.org/0000-0003-0097-4414

Ignas A. G. Snellen https://orcid.org/0000-0003-1624-3667

Matteo Brogi https://orcid.org/0000-0002-7704-0153

Jayne L. Birkby https://orcid.org/0000-0002-4125-0140

1. Received September 2022
2. Accepted September 2022
3. Published September 2022

Brown dwarfs; Exoplanet atmospheres

Abstract

Chemical and isotopic composition provide insights into the formation and evolution history of planets and brown dwarfs. Recent measurements of $^{12}CO/^{13}CO$ abundance ratios in the atmosphere of the young super-Jupiter YSES-1b and the isolated brown dwarf 2MASS J03552337+1133437 may point to distinct formation pathways. Here we present our analysis of 0.5 hr of science verification observations using the recently upgraded CRIRES spectrograph at ESO's Very Large Telescope on the same brown dwarf, with the aim to detect $C^{18}O$ and determine the $^{16}O/^{18}O$ isotope ratio. Our free retrieval analyses confirm the previous measurement of the carbon isotope ratio, and the inclusion of the $C^{18}O$ molecule in our models enables an initial tentative constraint of $^{16}O/^{18}O = 1489^{+1027}_{-426}$ on the oxygen isotope ratio, but this requires more data to be confirmed. These short observations showcase the prospect of studying the isotope inventory in brown dwarfs and super-Jovian exoplanets with high-dispersion spectroscopy.

1. Introduction

Studying atmospheric compositions of brown dwarfs and extra-solar planets provide opportunities to unveil their formation history. In addition to elemental abundance ratios (such as C/O), isotopologue ratios have been suggested to be informative probes for formation mechanisms of giant exoplanets and brown dwarfs (Molliere et al. 2019; Zhang et al. 2021b). Recently the $^{12}CO/^{13}CO$ abundance ratio was measured in the atmosphere of a super-Jupiter YSES-1b (∼31) and a young isolated brown dwarf 2MASS J03552337+1133437 (∼97) using medium- or high-resolution emission spectra (Zhang et al. 2021a, 2021b). Despite the similar mass, temperature, and retrieved C/O ratio, the super-Jupiter and the brown dwarf show distinct carbon isotopologue ratios, arguably

pointing to different formation pathways. Similar ^{13}CO-enrichment was also suggested in the atmosphere of the hot-Jupiter WASP-77Ab (Line et al. 2021). These measurements suggest a potential for carbon isotopologue ratio as a probe for planet formation, and calls for further observations of other planetary-mass objects and potentially other isotopes.

In addition to carbon, oxygen isotopes showing variations in solar system objects may also be informative for planet formation (Owen & Encrenaz 2003). The solar oxygen isotope ratio ^{16}O/^{18}O is ∼500 (Wilson 1999), hence more challenging to probe than carbon-13. With the commissioning of the upgraded cryogenic high-resolution cross-dispersed infrared echelle spectrograph (CRIRES) at the Very Large Telescope (VLT) (Kaeufl et al. 2004; Dorn et al. 2014), we aimed to take advantage of its high spectral resolving power to further characterize the atmosphere of the brown dwarf 2M0355, unveiling not only the carbon isotopes but also the oxygen isotope ^{18}O, following the same approach as presented in Zhang et al. (2021a). The inventory of different isotopes measured in this benchmark brown dwarf will benefit future comparisons with super-Jovian exoplanets to assist our understanding of planet formation.

2. Methods

We obtained high-resolution ($\mathcal{R} = \lambda/\Delta\lambda \sim 80{,}000$) emission spectra of 2M0355 at the *K*-band as part of science verification observations with the upgraded CRIRES at the VLT on 2021 September 19 under ESO programme 107.22TG. The observations were performed in seeing-limited mode with a standard ABBA nodding pattern, resulting in 4 science exposures of 300 s each. The data were taken at an airmass of 1.25 and a seeing of 0.″5. The sky transparency is sub-optimal with variable, thick clouds.

The raw data were first reduced using the CRIRES pipeline to correct for bias, flat fielding, sky background, and bad pixels. We then used the intermediate data products to optimally extract the spectrum, taking into account the curvature of the spectral trace on the detectors. The wavelength solution was calibrated against a telluric transmission model generated with ESO sky model calculator SkyCalc [6] (Noll et al. 2012). We corrected for telluric absorption lines using Molecfit (Smette et al. 2015), and shifted the spectrum to the target's rest frame.

Following the approach as presented in Zhang et al. (2021a), we carried out free retrieval analyses on the spectrum using a Bayesian framework composed of the radiative transfer tool petitRADTRANS (pRT) (Molliere & Snellen 2019) and the nested sampling tool PyMultiNest (Buchner et al. 2014). In addition to the VLT/CRIRES data presented here, we also included the archival spectrum taken with the near-infrared spectrograph Keck/NIRSPEC ($\lambda/\Delta\lambda \sim 25{,}000$) for a joint retrieval. Further information of the observation and data reduction can be found in Zhang et

al. (2021a). As the accurate calibration of the broad-band spectral feature is challenging in high-resolution observations, we discarded the absolute flux information by removing the low-frequency variation in both observations and models using a Gaussian smoothing filter with a width of 2 nm, only preserving the line-by-line variations.

We included in our fit the near-infrared (2MASS and WISE) photometric measurements (Faherty et al. 2016) to assist constraints on the radius, temperature and surface gravity. The photometry was converted from magnitudes to fluxes using the species package [7] (Stolker et al. 2020). We observed in this analysis that the high-resolution spectra were more constraining than the photometric points, to the point where our retrieval would not correctly fit the SED if equal weighting is assigned to the photometry and the high-resolution data. On the other hand, we found that scaling the log-likelihood of the photometric data points by a factor of 100 ($\sim\sqrt{\mathcal{R}_{\rm high}/\mathcal{R}_{\rm photom}}$) produced a good fit of both data sets. Although the validity of the procedure remains to be further studied, we note that the different weighting does not significantly affect the resulted isotopic ratios.

3. Results

The observed spectra at 2.32–2.37 μm and the best-fit model are shown in panel a in Figure 1. The retrieved posterior distribution of the isotope ratios are shown in panel c and d. The cross-correlation functions (CCF) with the ^{13}CO and C^{18}O templates are shown in panel b. We confirmed the previous detection of ^{13}CO as suggested by the CCF peak at zero velocity, and obtained a consistent and tighter constraint on the carbon isotope ratio ^{12}CO/^{13}CO = 108 ± 10. As for the oxygen isotope ratio, the retrieval provided a tentative constraint of ^{16}O/^{18}O = 1489^{+1027}_{-426}. The value is higher than the typical ratio (∼500) found in the solar system or local interstellar medium (Wilson 1999), while comparable to the measurements towards several young stellar objects (YSOs) (Smith et al. 2015) and an M dwarf binary (Crossfield et al. 2019). We refrain from further interpretation of the provisional measurement of the oxygen isotope ratio, as we did not detect the C^{18}O in the cross-correlation analysis, indicating that S/N $\lesssim$ 2. This is likely attributed to the lower than expected signal-to-noise ratio of the CRIRES spectrum due to the far from optimal observing condition. Nevertheless, the tentative constraint of the oxygen isotope ratio in the brown dwarf suggests the prospect of exploiting the isotope inventory in sub-stellar objects with future data of higher quality.

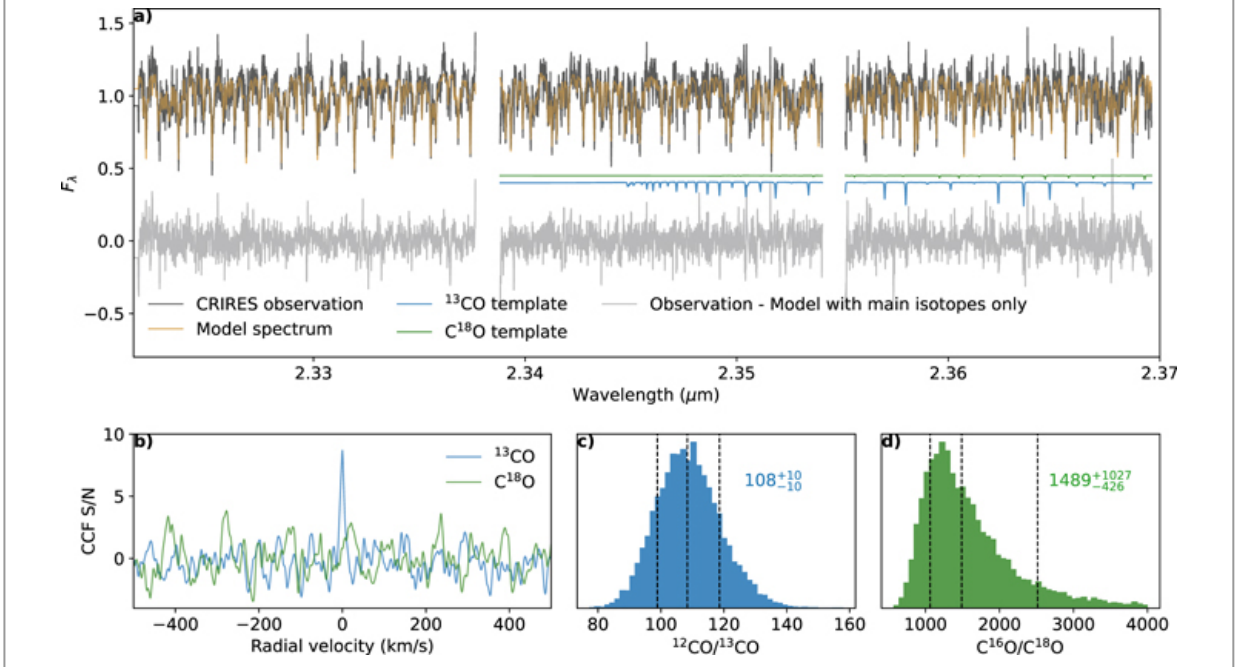

Figure 1. Panel (a): *K*-band (2.32–2.37 μm) spectrum of the brown dwarf 2M0355 taken with VLT/CRIRES. The orange line shows the best-fit model obtained through the retrieval analysis. The blue and green lines are the template spectra of ^{13}CO and C^{18}O. The observational residuals (namely, observations minus the model with main isotopes only) are shown in gray. Panel (b): Cross-correlation functions of the observational residuals with the ^{13}CO or C^{18}O template. Panel (c): Posterior distribution of the carbon isotope abundance ratio constrained by the retrieval. The vertical dashed lines denote the 1σ interval. Panel (d): Same as panel (c), but for the oxygen isotope ratio.

Based on observations collected at the European Southern Observatory under ESO programme 107.22TG. Y.Z. and I.S. acknowledge funding from the European Research Council (ERC) under the European Union's Horizon 2020 research and innovation program under grant agreement No 694513. M.B. acknowledges support from the STFC research grant ST/T000406/1. JLB acknowledges funding from the European Research Council (ERC) under the European Union's Horizon 2020 research and innovation program under grant agreement No 805445.

Footnotes

6 https://www.eso.org/observing/etc/skycalc

7 https://species.readthedocs.io/

↑ Buchner J., Georgakakis A., Nandra K. *et al.* 2014 *A&A* **564** A125

ADS Crossref Google Scholar

 Link to your libraries resources. Opens new window.

↑ Crossfield I. J. M., Lothringer J. D., Flores B. *et al.* 2019 *ApJL* **871** L3
ADS Crossref Google Scholar

 Link to your libraries resources. Opens new window.

↑ Dorn R. J., Anglada-Escude G., Baade D. *et al.* 2014 *Msngr* **156** 7
ADS Google Scholar  Link to your libraries resources. Opens new window.

↑ Faherty J. K., Riedel A. R., Cruz K. L. *et al.* 2016 *ApJS* **225** 10
ADS Crossref Google Scholar

 Link to your libraries resources. Opens new window.

↑ Kaeufl H. -U., Ballester P., Biereichel P. *et al.* 2004 *SPIE, Vol. 5492, Ground-based Instrumentation for Astronomy* ed A. F. M. Moorwood and M. Iye 1218
ADS Crossref Google Scholar

 Link to your libraries resources. Opens new window.

↑ Line M. R., Brogi M., Bean J. L. *et al.* 2021 *Natur* **598** 580
ADS Crossref Google Scholar

 Link to your libraries resources. Opens new window.

↑ Molliere P. and Snellen I. A. G. 2019 *A&A* **622** A139
ADS Crossref Google Scholar

 Link to your libraries resources. Opens new window.

↑ Molliere P., Wardenier J. P., van Boekel R. *et al.* 2019 *A&A* **627** A67
ADS Crossref Google Scholar

 Link to your libraries resources. Opens new window.

↑ Noll S., Kausch W., Barden M. *et al.* 2012 *A&A* **543** A92
ADS Crossref Google Scholar

 Link to your libraries resources. Opens new window.

↑ Owen T. and Encrenaz T. 2003 *SSRv* **106** 121
ADS Crossref Google Scholar

 Link to your libraries resources. Opens new window.

↑ Smette A., Sana H., Noll S. *et al.* 2015 *A&A* **576** A77
ADS Crossref Google Scholar

 Link to your libraries resources. Opens new window.

↑ Smith R. L., Pontoppidan K. M., Young E. D. and Morris M. R. 2015 *ApJ* **813** 120
ADS Crossref Google Scholar

 Link to your libraries resources. Opens new window.

↑ Stolker T., Quanz S. P., Todorov K. O. *et al.* 2020 *A&A* **635** A182
ADS Crossref Google Scholar

 Link to your libraries resources. Opens new window.

↑ Wilson T. L. 1999 *RPPh* **62** 143
ADS Crossref Google Scholar

 Link to your libraries resources. Opens new window.

↑ Zhang Y., Snellen I. A. G. and Mollière P. 2021a *A&A* **656** A76
ADS Crossref Google Scholar

 Link to your libraries resources. Opens new window.

↑ Zhang Y., Snellen I. A. G., Bohn A. J. *et al.* 2021b *Natur* **595** 370
ADS Crossref Google Scholar

 Link to your libraries resources. Opens new window.

Export references: BibTeX RIS